

# EXPERIMENTAL AND NUMERICAL STUDY OF THE BREACHING OF AN EMBANKMENT DAM

Dupont E.<sup>(1)</sup>, Dewals B.J.<sup>(1,2)</sup>, Archambeau P.<sup>(1)</sup>, Erpicum S.<sup>(1)</sup> & Piroton M.<sup>(1)</sup>

<sup>(1)</sup>Department ArGEnCo, Laboratory of Applied Hydrodynamics and Hydraulic Constructions, Institute of Civil Engineering, University of Liege,  
Ch. des Chevreuils 1, B52/3+1, B-4000 Liege, Belgium  
phone: +32 4 366 95 36 ; fax: +32 4 366 95 58; e-mail: Emilie.Dupont@ulg.ac.be

<sup>(2)</sup> FNRS Postdoctoral researcher

## ABSTRACT

In the framework of the study of the collapse of an embankment dam following its overtopping, an experimental study of the progressive breaching of such a dam has been performed. The present laboratory tests enable to validate and to complete a numerical approach previously studied by the authors. The two-dimensional analysis of the breaching is carried out on a scale model in a flume. A cross-section of a dam is scaled according to proper similarity rules, both for the flow and for the solid transport. The originality of the approach lies in the interaction between the experimental and numerical work. The experiments on the scale model are filmed in order to determine the time evolution of the dam profiles. The cross sections are extracted from the films and analyzed by an image-processing algorithm specifically developed for this application. These results are integrated into the hydrodynamic model WOLF2D, which computes the flow generated by the given transient topography and eventually supplies the relevant hydraulic parameters characterizing the dam breaching.

*Keywords:* dam breaching, embankment dam, model, experimental study

## 1 INTRODUCTION

When a dam break occurs upstream of a complex or a cascade of dams, the induced flows usually affect the dams located downstream. Therefore, it is only relevant to perform the risk analysis of such complexes in their whole. The embankment rockfill dam (dam n°2) mentioned below is part of a complex of two main dams and three secondary dams (Figure 1-1). The main dam (dam n°1), a 50 meter high concrete dam (Figure 1-2) is located upstream of the complex. The second one (dam n°2), an embankment rockfill dam (Figure 1-3), located 1.5 km downstream, constitutes the downstream limit of the complex. The role of the three secondary dams is simply to regulate the level of their upstream reservoir and so to enable the tourist function of the complex.

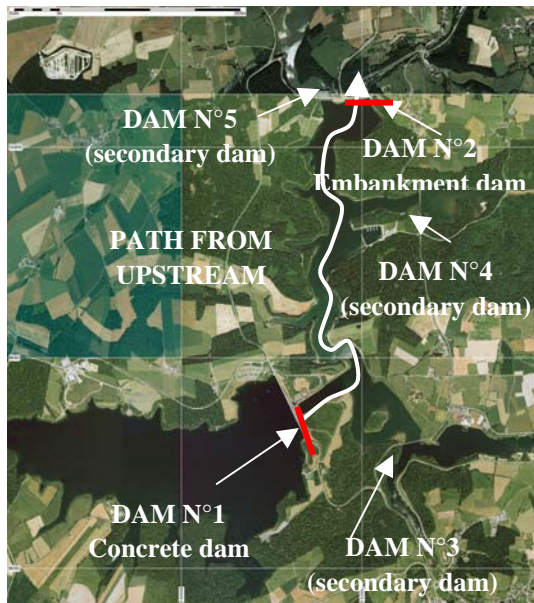


**Figure 1-1 : Aerial view of the complex of five dams**

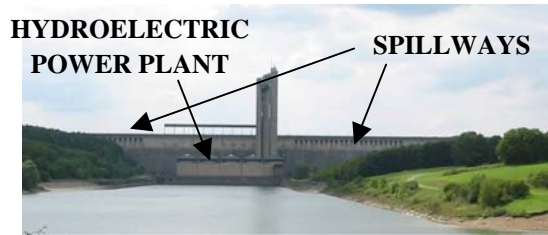


**Figure 1-2 : Dam n°1 seen from downstream**

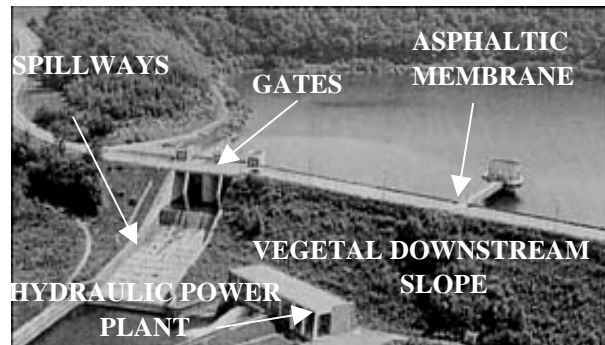


**Figure 1-3 : Dam n°2 seen from downstream**

A previous numerical study carried out by the authors evaluates the hydraulic consequences of an instantaneous collapse of the main dam (dam n°1) on the other structures of the complex and on the downstream valley [8; 9]. It reveals that the highest wave resulting from this incident causes a six meters elevation of the reservoir upstream of the dam n°2 (located 1.5 km downstream the dam n°1, Figure 1-1). Hence, the embankment dam (dam n°2) is overtopped. Such an incident on an embankment dam can dramatically damage or even completely wash it out. So the wave propagation in the downstream valley has been simulated, in this previous numerical study, with assumptions on the breaching parameters of the dam n°2 in accordance with empirical formulae. Those assumptions are validated here by means of the physical model of a cross section (2D study in a vertical plane) of the dam n°2, realized in order to confirm the breaching modeling and to complete the numerical study. The present paper describes this second part of the study [4; 10].

## 2 SCALING OF THE MODEL

A scale model of a cross section of the dam n°2 is built in a flume in order to simulate the overtopping of this embankment dam. The aim is to determine the time evolution of the shape of the dam n°2 during the breaching. The experiments are focused on the time evolution of the cross section of the scale model. To set up relevant and accurate relations between the obtained results on the scale model and the real dam (called the prototype), the scaling is performed according to proper similarity rules.

### 2.1 SIMILARITY RULES

Two physical processes have to be scaled: the flow through the hydrodynamic similarity and the sediment transport by the sedimentary similarity. Indeed, sediment transport is a governing factor in the breaching mechanism of such an embankment dam.

From the hydraulic point of view, the flow conditions have to be similar on the scale model and on the real situation. The dimensional analysis emphasizes five non-dimensional

numbers characterizing the flow, called Froude Fr, Reynolds Re, Euler Eu, Weber We and Cauchy Ca numbers:  $Fr = \frac{V}{\sqrt{gL}}$ ;  $Re = \frac{LV}{\nu}$ ;  $Eu = \frac{\rho V^2}{\Delta P}$ ;  $We = \frac{\rho L V^2}{\sigma}$  and  $Ca = \frac{\rho V^2}{E_b}$  (1)

where  $V$  = flow velocity;  $L$  = characteristic length of the flow;  $g$  = gravity acceleration;  $\nu$  = fluid kinematic viscosity;  $\rho$  = fluid density;  $P$  = pressure;  $\sigma$  = fluid surface tension and  $E_b$  = elasticity volumetric modulus of the fluid.

The breaching due to overtopping is a free surface process dominated by gravity phenomena. Therefore the Froude similarity must be respected. This requires that the ratio between the gravity and the inertia forces (which is the Froude number Fr) are both equal in the model and in the prototype.

Furthermore, to ensure that the viscosity effects remain insignificant, the Reynolds number must be higher than 1500 for both the scale model and the prototype [7].

From the sedimentary point of view, the similarity rules require that four non-dimensional numbers are kept equal on the scale model and on the prototype. Those four numbers are the non-dimensional shear stress  $\tau_*$ , the particle Reynolds number  $Re_*$ , the

$$\text{geometric ratio and the relative density s: } \tau_* = \frac{\rho U_*^2}{(\rho_s - \rho)gd}; Re_* = \frac{U_* d}{\nu}; \frac{h}{d}; s = \frac{\rho_s}{\rho} \quad (2)$$

where  $\rho$  = fluid density;  $\rho_s$  = sediment density;  $U_*$  = shear velocity;  $g$  = gravity acceleration;  $d$  = sediment diameter;  $\nu$  = water kinematic viscosity and  $h$  = flow depth.

The sediment transport is, in this kind of breaching, dominated by the bed load transport. The main characteristic of this sediment transport mechanism is the non-dimensional shear stress  $\tau_*$ . Both the non-dimensional shear stress  $\tau_*$  and the particle Reynolds number  $Re_*$  can not be conserved simultaneously. So, the non-dimensional numbers are all simulated exactly except for the particle Reynolds number. However, its value is kept higher than the critic threshold of 70, to ensure the viscosity force being sufficiently weak [7].

The scale ratios  $\lambda$  are defined as the ratios between a prototype characteristic and the same characteristic observed on the scale model. They are developed below for the similarity rules explained before. The index  $p$  and  $m$  refer respectively to the prototype and to the scale model.

$$\text{From the hydraulic point of view: } \lambda_{Fr} = \frac{\frac{V_p}{\sqrt{g_p L_p}}}{\frac{V_m}{\sqrt{g_m L_m}}} = \frac{\lambda_v}{\lambda_g^{1/2} \lambda_L^{1/2}} = 1 \Rightarrow \boxed{\lambda_v = \lambda_L^{1/2}} \quad (3)$$

with  $\lambda_{Fr} = 1$  (to conserve the Froude number) and  $\lambda_g = 1$  (gravity acceleration equal in the scale model and in the prototype).

$$\lambda_T = \frac{\lambda_L}{\lambda_v} \Rightarrow \boxed{\lambda_T = \lambda_L \lambda_L^{-1/2} = \lambda_L^{1/2}} \quad (4)$$

$$\lambda_Q = \lambda_v \lambda_L^2 \quad \Rightarrow \quad \boxed{\lambda_Q = \lambda_L^{1/2} \lambda_L^2 = \lambda_L^{5/2}} \quad (5)$$

$$\text{From the sedimentary point of view: } \lambda_{\tau_*} = \frac{\frac{\rho_p U_{*p}^2}{(\rho_{s,p} - \rho_p) g_p d_p}}{\frac{\rho_m U_{*m}^2}{(\rho_{s,m} - \rho_m) g_m d_m}} = \frac{\lambda_{U_*}^2}{\lambda_{\Delta\rho/\rho} \lambda_g \lambda_d} = 1, \quad (6)$$

with  $\lambda_{\tau_*} = 1$  (to conserve the non-dimensional shear stress);  $\lambda_g = 1$  and  $\Delta\rho/\rho = (\rho_s - \rho)/\rho$ .

$$\Rightarrow \quad \lambda_{U_*}^2 = \lambda_{\Delta\rho/\rho} \lambda_d \quad (7)$$

Darcy-Weisbach formula [5; 6; 12] gives  $\lambda_{U_*} = \lambda_v \lambda_f^{1/2}$

where  $f$  is the frictional coefficient,  $\lambda_f \approx 1$  (see Table 2-2) and  $\lambda_v = \lambda_L^{1/2}$  as stated by equation (3).

$$\text{As a result, we obtain:} \quad \lambda_d = \lambda_{\Delta\rho/\rho}^{-1} \lambda_L \quad (8)$$

To conserve also the geometric ratio, it comes:

$$\lambda_{h/d} = \frac{\lambda_h}{\lambda_d} = 1 \quad \Rightarrow \quad \lambda_d = \lambda_h \quad \Rightarrow \quad \boxed{\lambda_d = \lambda_L} \quad (9)$$

$$\text{In conclusion, equations (8) and (9) lead to} \quad \boxed{\lambda_{\Delta\rho/\rho} = 1} \quad (10)$$

Three of the four non-dimensional numbers linked to the sediment dimensional analysis are therefore conserved.

## 2.2 APPLICATION TO THE DAM N°2

The dam n°2 is about 18 meters high ( $L_p$ ). The width is 14.2 meters ( $b_p$ ) at the crest and 82 meters at the base ( $B_p$ ). The dam is assumed to be overtopped by 2.5 meters ( $H_p$ ). The similarity laws are applied to optimally exploit the laboratory facilities (Figure 2-1).

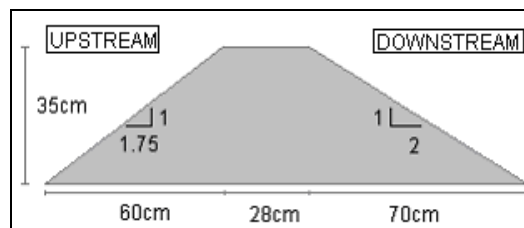


Figure 2-1 : Scale model profile

The flow leading to this overtopping is estimated by the broad-crested-weirs formula [5; 6; 12].

As shown by Table 2-1, the Reynolds number is indeed high enough to ensure that the viscosity effects remain insignificant [7].

Since the grain size distribution of the dam n°2 is completely non uniform and not known accurately, the sediment grain size is assumed to be 0.2 m for the experiments. A sensitivity

analysis of this parameter must be carry out to determine its influence. The sediment density is estimated at 2750 kg/m<sup>3</sup>.

The sediment density of the scale model and the sediment size are given by

$$\rho_{s,m} = \rho_{s,p} = 2750 \text{ kg/m}^3; d_m = \frac{d_p}{\lambda_L} \quad (11)$$

This scaling is in accordance with the constraint on the particle Reynolds number (Table 2-2).

**Table 2-1 : Verification of the Re condition**

	Prototype	Model
V (m/s)	2.696	0.376
L (m)	2.5	0.049
Re (1)	$6.7 \cdot 10^6 > 1500$	$1.8 \cdot 10^4 > 1500$

**Table 2-2 : Verification of the Re\* condition**

	Prototype	Model
V (m/s)	2.696	0.376
f (m <sup>1/2</sup> /s)	0.05	0.05
d (m)	0.2	0.0038
Re* (1)	$42 \cdot 10^3 > 70$	$115 > 70$

However, although the respect of requirements is assured, the particle Reynolds numbers differ by more than two orders of magnitude. For this reason, a second scaling is envisaged, in order to increase the particle Reynolds numbers of the scale model by selecting a suitable sediment density. This approach allows only the conservation of the non-dimensional shear stress and not the three others numbers.

Such an approach leads for instance to the density values and the corresponding sediment diameters mentioned in Table 2-3.

**Table 2-3 : Sediment properties and Re\* of the second application of similarity rules**

Sediment density (kg/m <sup>3</sup> )	Sediment diameter (mm)	Re* (model)
1700	9.7	287
1900	7.6	223
2200	5.7	167

### 3 EXPERIMENTS

#### 3.1 LABORATORY DEVICE

The experiments are carry out in a 30 meters long flume (Figure 3-1). A silting basin is located at the downstream end of the flume. Two probes are placed upstream of the model and one downstream. A video camera faces the cross profile of the dam and an other one faces the downstream slope. The experiments are lead in properly controlled brightness conditions.

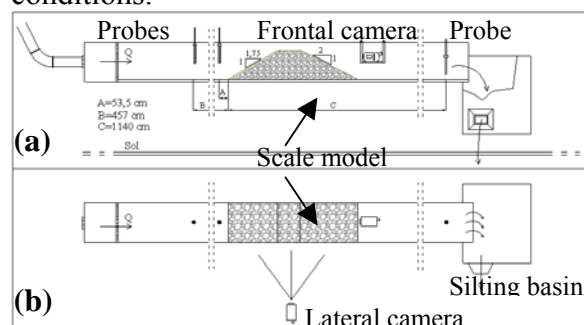


**Figure 3-1 : (a) Side view of the laboratory installation, showing the three probes and the frontal camera; (b) Aerial view showing both cameras**

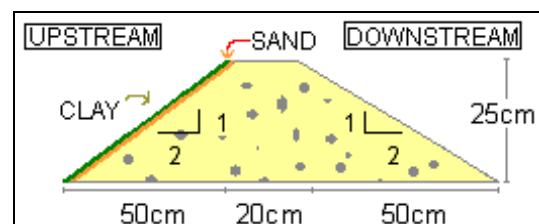


**Figure 3-2 : Second scale model**

Two series of experiments are carry out. The first one, including five experiments, corresponds to the scale model, the solid material and the flow condition, which have been determined in section 2.2 (Figure 2-1). The scale model body is made of 2-4 mm limestone gravel.

The second series of experiments includes two tests. This second modeling does not fulfill to the similarity rules mentioned above (Figure 3-2) because the aim is more qualitative, as will be detailed later. The model is made of gravel (2-7 mm limestone gravel) and sand mixing (2 volumes of gravel for 1 of sand). The mixing is put by successive compacted layers of about 5 cm. Moreover, the flow is increased up to the value of 0.014 m<sup>3</sup>/s.

The upstream slope of the dam n°2 is protected by an asphaltic membrane (Figure 1-3). The challenge lies in creating on the scale model an efficient watertightness without introducing intrusive rigidity in the modeling. Therefore, this watertightness is modeled on the two types of experiments by a thin clay layer (mixing of clay powder and water) put on a 1 cm thick sand layer placed on the upstream face of the scale model (Figure 3-2). The sand layer ensures the transition between the clay and the gravels in order to avoid the penetration of the thin clay sediment into the body of the dam, which would induce artificial cohesion. Only the last experiment of the second series is lead with a different watertightness: the sand layer is not used in order to decrease the effect of intrusive rigidity.



**Figure 3-3 : System of watertightness**

The physical model in accordance with the second scaling (section 2.2) has not been modeled yet. The difficulty of this modeling lies in the selection of a suitable material. This range of density is indeed badly covered by available material. Moreover, the particle size can not be increased without becoming of the same order of magnitude as the overtopping height. As a consequence increasing perturbations linked to scale effects would be expected. However, it will be interesting to carry out such experiments in the future.

### **3.2 EXTRACTION OF THE RESULTS**

The time evolution of the dam profile is extracted from the films (of the lateral camera, Figure 3-1) of the scale model and exploited by an original image-processing algorithm, specifically developed by the authors for the present application.

The whole breaching hydrograph is indirectly estimated: the time evolution of the dam profiles is integrated into the hydrodynamic model WOLF2D [1-3; 11] which computes the flow generated by the given transient topography and determines the time evolution of the outflow discharge. The friction coefficient is calibrated by the comparison with water depths measured by the three resistive probes during the experiments.

### 3.3 DESCRIPTION OF THE EROSIVE PROCESS

The clay layer ensures the watertightness of the scale model until the water exceeds the crest level. Then, the water seeps through the scale model, forming a thin hole (Figure 3-4). The seepage spreads within the body of the model until it reaches the downstream slope.



Figure 3-4 : Hole in the crest

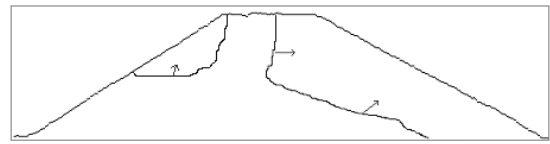


Figure 3-5 : Watertightness spread

A sliding is then observed at the lower part of the downstream slope. This sliding just follows the actual overtopping. The motion progresses from the downstream face to the upstream one, the downstream slope rotating around a pivot point (Figure 3-6). The pictures of Figure 3-6 illustrate, by means of several successive cross sections of the scale model, the time evolution of the sliding.

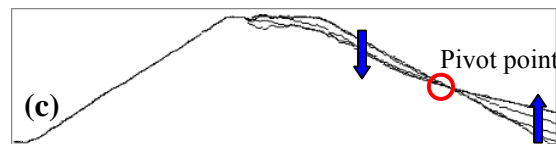
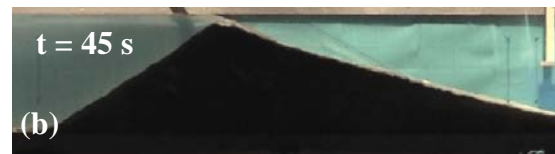
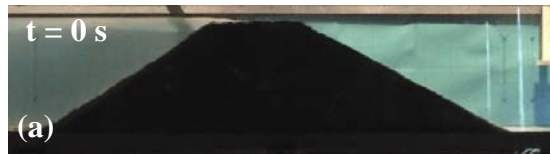


Figure 3-6 : (a) Initial profile; (b) Sliding of the downstream slope; (c) Rotation of the downstream face around the pivot point, superposition of the cross sections obtained by the image processing tool

Then, the flow on the crest forms a jet (partly aerated) which progressively intensifies the crest erosion. Antidunes can be observed on the downstream face (Figure 3-7). The cross section ends up stabilizing without a complete washout of the dam (Figure 3-8).

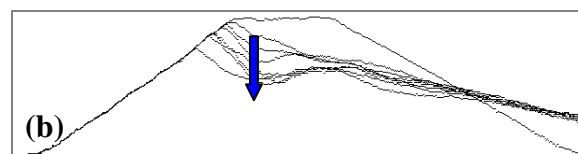
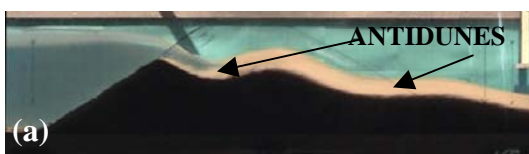


Figure 3-7 : (a) Cross section of the scale model; (b) Crest lowering, superposition of the cross sections obtained by the image processing tool

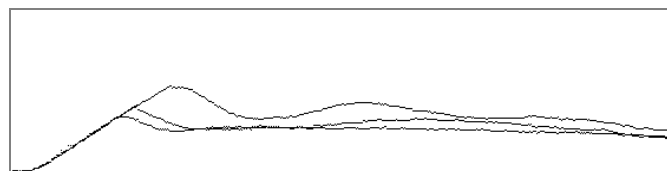


Figure 3-8 : Cross section stabilizing, superposition of the cross sections obtained by the image processing tool

The second camera installed in front of the downstream slope enables to monitor the breach formation more in details. Most experiments show an uniform erosion of the crest in

the lateral direction. The crest level decreases uniformly on the whole width of the scale model. In some cases, a 3D breach is observed. This effect depends on the care and precision of the material installation, as well as the uniformity of the compacting. These observations show limitations of the 2D study (in the vertical plane).

When a breach occurs, the erosive processes are mainly similar to those previously mentioned, with modified erosion process of the crest. The flow induces a breach starting in the middle of the crest which rapidly progresses laterally. After the breach initiation, the sliding of the downstream slope progresses and the breach widens.

The first series of experiments described shows that when the water overtops the crest, the flow seeps into the dam. The initiation of the collapse is due to this seepage. A second series of experiments, is carry out in order to demonstrate qualitatively a breaching mechanism governing solely by overtopping and not by seepage anymore. Therefore, the second model is made more impermeable than the first one. That is ensured by a sand and gravel mixing (Figure 3-2). The working out method increases even more the mixing compactness, indeed, the mixing is put by successive compacted layers of about 5 cm. Moreover, the discharge is selected twice higher than in the previous experiments in order to reduce the relative effect of seepage.

This second type of experiments leads, as expected, to an overtopping without as much seepage as in the first type of tests. The overtopping effect on the stability can thus clearly be observed. The first experiment of this series shows a significant rigidity introduced by the waterproof layer upstream. To avoid this phenomenon, the sand layer is not placed in the last experiment any more. The overtopping leads to the erosion of the downstream slope from the toe towards upstream. It is eroded towards the upstream side of the crest. Slope breaks on the downstream slope are observed while the erosion progresses (Figure 3-9). Finally, the downstream slope erosion combines with the crest erosion (Figure 3-10). The erosion occurs uniformly on the width. At the end of the breaching, the scale model forms a triangular mound (Figure 3-11).

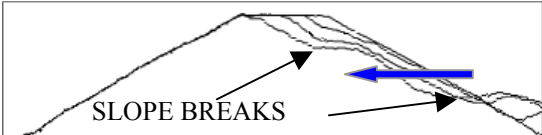


Figure 3-9 : Erosion toward upstream slope

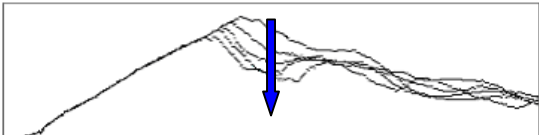


Figure 3-10 : Crest erosion

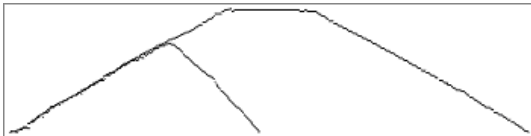


Figure 3-11 : Superposition of the initial and final cross section, second type of experiments

**3.4 DISCUSSION OF THE RESULTS**

The image processing algorithm enables to highlight conclusions about the time evolution of the erosion. For the first type of experiments, it has been observed that the volume under the crest decreases in two successive linear stages: a first quick stage is followed by a crest erosion about seven time slower (Figure 3-12). For the second type of experiments, the evolution of the volume of eroded material increases more gradually, in one linear stage.

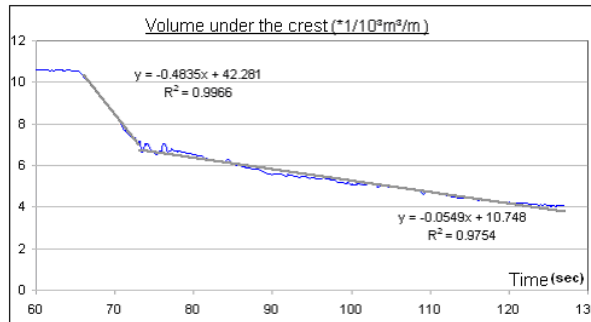


Figure 3-12 : Time evolution of the material volume, first type of experiments

#### 4 DISCHARGE EVALUATION

The time evolution of the cross section of the scale model is introduced into the hydrodynamic model WOLF2D. This software provides the flow hydrograph resulting of this transient topography. The parameters affecting the flow are calibrated by comparing the probe measurements and the water depths provided by the hydrodynamic simulations (Figure 4-1).

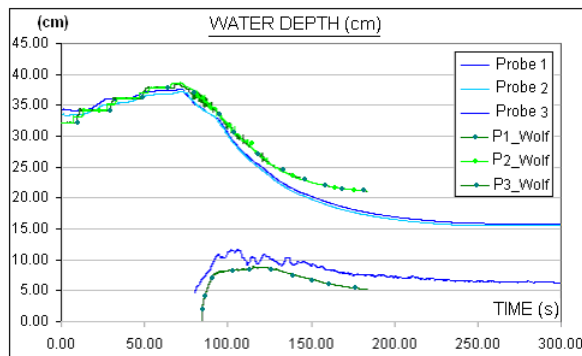


Figure 4-1 : Comparison of the water depths Laboratory – WOLF 2D

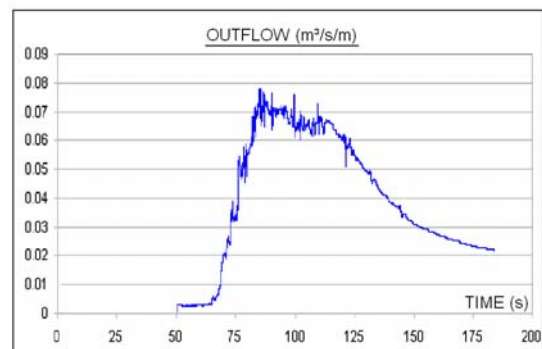


Figure 4-2 : Outflow discharge on the scale model at the level of the crest

The computed flow characteristics can be converted into values for the prototype by means of the similarity laws. The outflow peak discharge on the prototype is  $Q_p = q_m \cdot \lambda_q \cdot L = 5089 \text{ m}^3/\text{s}$  where  $Q_p$  = peak discharge of the flow on the dam  $n^2$  during the breaching;  $q_m$  = specific peak discharge on the model;  $\lambda_q$  = scale ratio of the specific discharge;  $L$  = breach width, which is estimated at about 150 m by the empirical formulas [4; 9; 10].

The following comments may be formulated:

- In the above simulations, the seepage process is not taken into account. However, this phenomenon does not affect the peak discharge significantly, as confirmed by several empirical formulae [13].
- In the scenario (less probable) where the breach stretches over the whole dam width ( $L = 250 \text{ m}$ ), the peak outflow would reach  $8482 \text{ m}^3/\text{s}$ .
- The peak discharge determined presently by the interaction between experimental measurements and numerical modeling is in satisfactory agreement with the values provided by empirical formulae [8-10] (about  $5000 \text{ m}^3/\text{s}$  for a 150 m breach width).

Moreover, this outflow peak discharge occurs 8.4 min after the overtopping :

$$T_{P,\text{peak}} = T_{m,\text{peak}} \lambda_T$$

where  $T_{P,\text{peak}}$  = time of the outflow peak discharge after the overtopping on the prototype;  
 $T_{m,\text{peak}}$  = time of the outflow peak discharge after the overtopping measured on the model and  
 $\lambda_T$  = scale ratio of time.

The breaching duration for the experiments is about 2 min, which leads to a value of 14 min for the dam n°2 :  $T_{p,breaching} = T_{m,breaching} \cdot \lambda_T$   
 Furthermore, the flow velocities on the downstream slope of the dam n°2 reach about 12.5 to 13 m/s.

## 5 CONCLUSIONS

The present paper comprehensively describes the scaling method and the experiments details of the laboratory model of a cross section of an embankment dam, which is submitted to an overtopping. The experiments validate the breaching mechanism adopted by the authors in a comprehensive risk assessment study on a complex of five dams [8; 9]. Data measured during the experiments are integrated as a transient topography in the hydrodynamic software WOLF2D, in order to evaluate the flow pattern upstream and downstream of the dam. This original coupling of the numerical study and the experimental work has shown the complementarity and the power of the interactions between those two approaches.

## 6 BIBLIOGRAPHY

- [1] Archambeau, P., Dewals, B., Detrembleur, S., Ercicum, S., and Piroton, M. (2004). "A set of efficient numerical tools for floodplain modeling." *Shallow Flows*, W. S. J. Uijtewaal, ed., Balkema, Leiden, etc, 549-557.
- [2] Archambeau, P., Dewals, B., Ercicum, S., Detrembleur, S., and Piroton, M. (2004). "New trends in flood risk analysis: working with 2D flow models, laser DEM and a GIS environment." *Proc. 2nd Int. Conf. on Fluvial Hydraulics: River Flow 2004*, R. Della Morte, ed., Balkema, Leiden, etc., 1395-1401.
- [3] Archambeau, P., Ercicum, S., Dewals, B., Detrembleur, S., Duy, B. K., and Piroton, M. "Modern techniques for flood risk analysis: quasi-3D simulations in a GIS environment." *European Geosciences Union - General Assembly*, Vienne, Autriche, 3.
- [4] Bonsignori, M. (2005). "Analyse sur modèle physique des modes de rupture d'un barrage en enrochements," *Travail de fin d'études*, Université de Liège et Università di Pisa (Italie).
- [5] Chanson, H. (1999). *The Hydraulics of open Channel Flow*, Butterworth-Heinemann, Oxford.
- [6] Chaudhry, M. H. (1993). *Open-Channel Flow*, Prentice Hall, Englewood Cliffs.
- [7] Coleman, S. E., and Andrews, D. P. (2000). "Overtopping breaching of noncohesive homogeneous embankments," *The University of Auckland*, Auckland.
- [8] Dewals, B. (2006). "Une approche unifiée pour la modélisation d'écoulements à surface libre, de leur effet érosif sur une structure et de leur interaction avec divers constituants," *Thèse de doctorat*, Université de Liège.
- [9] Dewals, B. J., Archambeau, P., Ercicum, S., Detrembleur, S., and Piroton, M. "Comparative analysis of the predictive capacity of breaching models for an overtopped rockfill dam." *Proc. Int. Workshop "Stability and Breaching of Embankment Dams"*, Oslo, Norvège.
- [10] Dupont, E. (2005). "Etude de rupture d'un barrage hétérogène en enrochement," *Travail de fin d'études*, Université de Liège.
- [11] Ercicum, S., Archambeau, P., Dewals, B., Detrembleur, S., and Piroton, M. "Computation of the Malpasset dam break with a 2D conservative flow solver on a multiblock structured grid." *Proc. 6th Int. Conf. of Hydroinformatics*, Singapore.
- [12] Piroton, M., Archambeau, P., Dewals, B., Ercicum, S., and Mouzelard, T. (2002). *Cours d'Hydraulique Appliquée*, Université de Liège.
- [13] Robinson, K. M., E., P., Kadavy, K. C., and Rice, P. E. a. C. E. "Rock chutes on slopes between 2 and 40%." *ASAE Annual Int. Meeting*, Orlando, Florida.